Arabian Journal of Geosciences (2020) 13: 622
https://doi.org/10.1007/s12517-020-05353-3

ORIGINAL PAPER

Development of earthquake early warning system for Kachchh, Gujarat, in India using τc and P_d

Santosh Kumar[1] · Himanshu Mittal[2] · Ketan Singha Roy[1] · Yih-Min Wu[2,3] · Richa Chaubey[1] · Ajay Pratap Singh[4]

Received: 2 May 2018 / Accepted: 25 April 2020 / Published online: 9 July 2020

Abstract
Development of earthquake early warning system (EEWS) is in advanced stage in different parts of the world including India. The success of EEWS for mitigating seismic risk and saving human lives has been well documented in Mexico, Japan, and Taiwan, where the alert is issued to the public. Taking advantage of the recorded ground motion data from the network of Institute of Seismological Research (ISR), India, with magnitude range 3.0–5.2, we investigated correlations between various ground motion parameters like peak ground acceleration (PGA), peak ground velocity (PGV), peak ground displacement (PGD), P_a, P_v, P_d, and τ_c.Three- to 5-s time windows are considered to measure P_a, P_v, P_d, and τ_c from the vertical component of the waveforms. Linear regression analysis is performed at various time steps (3- to 5-s time interval). The results show that considering 4- and 5-s windows exhibits good relationships compared with the 3-s window, which shows more scattering. These empirical relationships using τ_c and M as well as P_d and M are very helpful in determining the earthquake magnitude and subsequently taking steps toward risk assessment.

Keywords Earthquake early warning (EEW) · Institute of Seismological Research (ISR) · P_d · τc · PGA · PGV · PGD · Seismic risk

Introduction

The success of earthquake early warning (EEW) for mitigating seismic risk and saving human lives has been well documented in Mexico, Japan, Taiwan, and other parts of the World. EEW is a process in which warning is issued before the arrival of strong ground shaking. Mexico and Japan are providing EEW alerts to the public (Allen et al. 2009; Kamigaichi et al. 2009; Wu et al. 2007). The EEW system of Mexico utilizes peak ground motion (PGM), to issue 60 s or more warning to the public in Mexico City (around 300 km away) from earthquake occurring near the Guerrero gap subduction zone (Anderson et al. 1995; Espinosa-Aranda et al. 1995). Japan uses more than 4500 instruments for real-time recording of earthquakes as well as for providing a warning (Hoshiba et al. 2008). Depending upon the location of occurrence of the earthquake, the warning time in Japan may range from a few seconds to 40 s. Taiwan provides warning alert to authorities and in recent time to public (Chen et al. 2015; Wu et al. 2016). In Taiwan, the Central Weather Bureau (CWB) is the official agency to issue the warning to authorities as well as the public. CWB uses about 400 instruments for real-time recording as well as issuing warning to the public. On the other hand, the National Taiwan University (NTU) uses a network of about 612 low-cost P-alert sensors for research purpose (Wu et al. 2013; Wu et al. 2019). There are two types of EEWS, namely onsite and regional (Kanamori 2005). Onsite warning may be provided using a single station or a small network of stations for one location. In this system, as soon as P-wave is recorded by the sensor, an alarm is generated at site and systems in close proximity may go for auto shutdown like nuclear power plants. A regional warning requires a dense seismic network near the epicentral zone and high-speed communication system, which can transmit the seismic signal within few seconds to Central Recording System (CRS). As seismic waves travel slower than

Responsible Editor: Narasimman Sundararajan

✉ Himanshu Mittal
himanshumitt10@gmail.com

1 Institute of Seismological Research, Gandhinagar, Gujarat, India

2 Department of Geosciences, National Taiwan University, Taipei 10617, Taiwan

3 Institute of Earth Sciences, Academia Sinica, Taipei, Taiwan

4 Ministry of Earth Sciences, Delhi, New Delhi, India

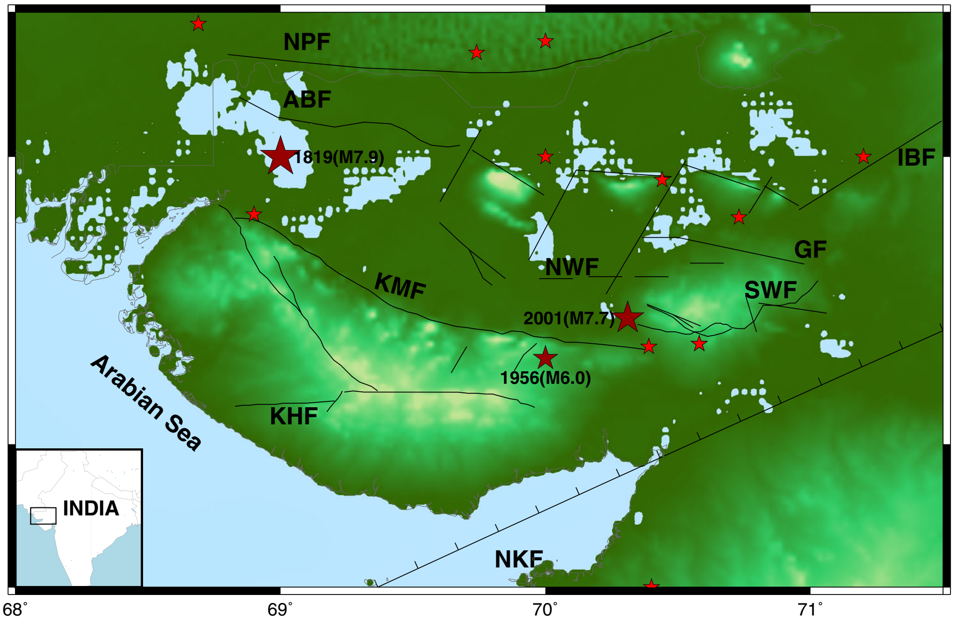

Fig. 1 Fault map of Kachchh, Gujarat. Major faults Katrol Hill Fault (KHF), Kachchh Mainland Fault (KMF), South Wagad Fault (SWF), Island Belt Fault (IBF), and Nagar Parkar Fault (NPF) are shown. The location of major earthquakes: 1819 Mw 7.8 Allah Bund earthquake and the 2001 Mw 7.7 Bhuj earthquake as well as some of other earthquakes having magnitude ≥ 6 are also shown

electromagnetic waves (for communication), using the data of the first few seconds (3–5 s), it is possible to provide the regional warning within 15 s. In general, in an onsite EEWS application, a single station can provide warning in regions without a seismic network and maximize warning time at sites close to the epicenter (Lockman and Allen 2005).

In regional EEW, determining earthquake magnitude is one of the crucial aspects, as this can be the sole parameter on the basis of which warning will be issued. However, determining magnitude from the initial few seconds of the waveform is not straight forward, as fault may be still rupturing. In this context, Wu et al. (1998) used a technique exploiting initial 10 s of signal to relate it with the local magnitude M_L. In another study, 22 s of signal data are used by Taiwan CWB to determine the earthquake parameters. Since shear waves travel at a speed of 3 km/s, this approach provides early warning for areas beyond 70 km only. Both these two approaches are purely empirical, whereas recent approaches based on peak displacement amplitude (P_d) and the characteristic

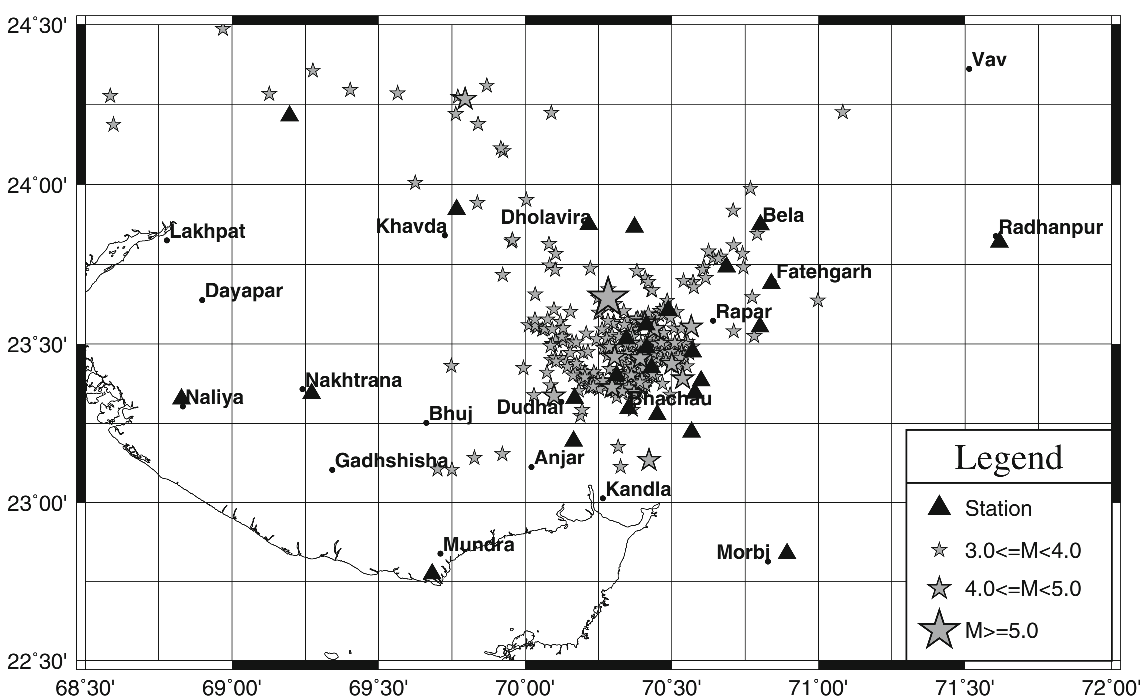

Fig. 2 Map showing the location of various earthquakes used in present study and stations recording these earthquakes

period (τ_c) look more appealing. These two parameters estimated from the initial few seconds (3–5 s) after P-wave arrival are used widely for determining whether an earthquake will be damaging or not. A P_d value larger than 0.5 cm and τ_c larger than 1 s are indicators of damaging earthquakes (Wu and Kanamori 2005a, 2008a). In addition, P_d is supposed to be a better indicator for the intensity of an earthquake than τ_c as the latter is more sensitive to the signal to noise ratio (SNR). P_d is a physical parameter and magnitude estimation using it seems more reasonable. As per Olson and Allen (2005), earthquake magnitude is controlled by the initial stages of the rupture, which justifies the effectiveness of P_d amplitude theory in EEW.

India is at risk of prevalence of high magnitude earthquake from the Himalayas in the north (Mittal et al. 2016a, 2016b) and northeast, Gujarat in west, and Andaman and Nicobar in the southern part of India. Following the probability of occurrence of the devastating earthquake in northern Himalayas, the Indian Institute of Technology, Roorkee (IITR), installed a network of 100 seismic stations for developing EEW system (Kumar et al. 2014). This network was installed based on the performance of strong motion instrumentation network in the Himalayas (Mittal et al. 2006; Kumar et al. 2012). This network is in operation and working perfectly. Despite its operation for the last 4 years, no big earthquake is recorded by this network to test the effectiveness of the network. Mittal et al. (2019a, 2019b) tested the performance of these 100 instruments' network using the recorded earthquakes from Taiwan and synthesized records. They found that in the event of an earthquake in the Himalayas, Delhi (the national capital of India) may have a lead time of 60 s. On the premise of performance of these 100 instruments, IITR is installing 100 additional instruments to have a wide coverage area.

The state of Gujarat is located in the westernmost part of the intraplate region of India. Gujarat being an industrial state is a hub of many petrochemical industries, oil industries, and ports. Gujarat is vulnerable to natural disasters like earthquakes and is of importance owing to increasing population. The Kachchh region of Gujarat has already witnessed two massive damaging earthquakes—1819 M_w 7.8 Allah Bund earthquake and the 2001 M_w 7.7 Bhuj earthquake within the span of 182 years (Johnston and Kanter 1990; Rastogi 2001). Additionally, the region has also experienced seven other $M \geq 6.0$ earthquakes (Quittmeyer and Jacob 1979; Rastogi 2001, 2004). The 2001 Bhuj earthquake in Kachchh region caused widespread damage in terms of fatalities and economic loss. The earthquake was so massive that damage was even witnessed in Ahmedabad, 240 km away from the epicenter, causing human lives as well as building collapse. Valuable human lives can be saved if timely earthquake alert is provided and individuals are very much prepared. To monitor the seismic activity and reporting in Gujarat state of India, the Institute of Seismological Research (ISR) in 2006 installed the Gujarat Seismic Network (GSNet) consisting 22 online broadband seismograph (BBS) stations and 40 offline strong motion accelerograph (SMA) (Chopra et al. 2008). Presently, data from 45 seismic stations is coming online via VSAT and 50 more SMAs are proposed to be

Table 1 Various attenuation relationships between various ground motion parameters for varying time windows (3–5 s)

Regression parameters	Time window	Regression coefficients		
		A	B	C
PGA and P_a	3 s	0.21	0.76	0.328
PGA and P_v		1.73	0.79	0.329
PGA and P_d		2.98	0.76	0.361
PGV and P_a		−1.60	0.73	0.341
PGV and P_v		−0.07	0.78	0.323
PGV and P_d		1.24	0.77	0.339
PGD and P_a		−3.16	0.72	0.389
PGD and P_v		−1.61	0.79	0.359
PGD and P_d		−0.18	0.80	0.349
τ_c and M		1.42	0.16	0.116
P_d and M		−7.62	1.03	0.404
PGA and P_a	4 s	0.17	0.76	0.305
PGA and P_v		1.68	0.78	0.304
PGA and P_d		2.93	0.76	0.336
PGV and P_a		−1.63	0.73	0.321
PGV and P_v		−0.13	0.77	0.301
PGV and P_d		1.17	0.77	0.315
PGD and P_a		−3.20	0.72	0.374
PGD and P_v		−1.68	0.78	0.342
PGD and P_d		−0.28	0.79	0.330
τ_c and M		1.39	0.15	0.116
P_d and M		−7.71	1.08	0.449
PGA and P_a	5 s	0.12	0.75	0.292
PGA and P_v		1.62	0.78	0.288
PGA and P_d		2.86	0.76	0.318
PGV and P_a		−1.68	0.73	0.310
PGV and P_v		−0.19	0.77	0.285
PGV and P_d		1.10	0.76	0.294
PGD and P_a		−3.24	0.72	0.367
PGD and P_v		−1.74	0.77	0.331
PGD and P_d		−0.36	0.79	0.312
τ_c and M		1.39	0.15	0.113
P_d and M		−7.70	1.10	0.453

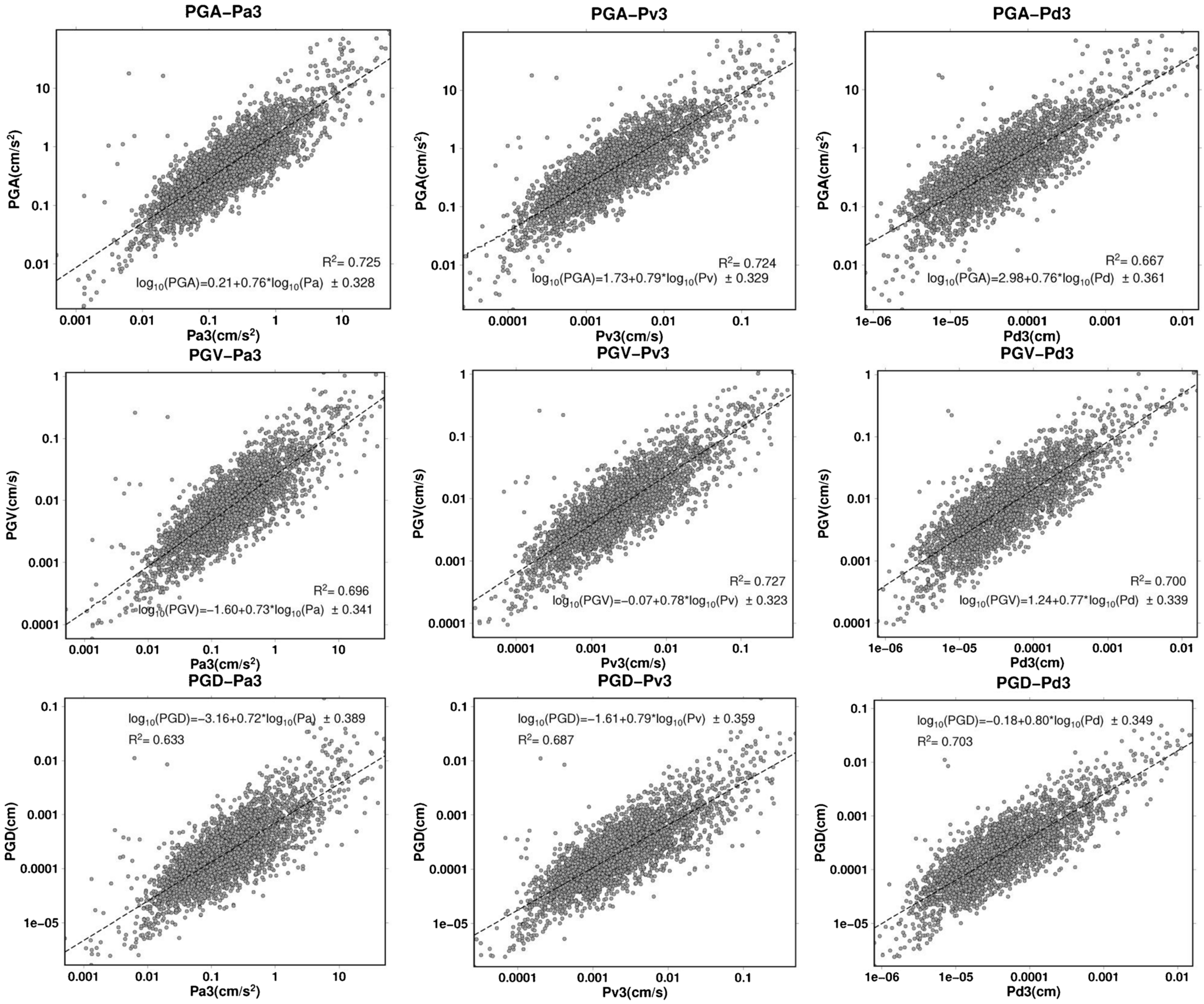

Fig. 3 Empirical relationships between ground motion parameters (PGA, PGV, PGD, P_a, P_v, P_d) for 3-s window after P-wave arrival. Pearson correlation coefficient (regression coefficient) is calculated between log10(PGM) and log10(Pm3), where $M = A$ (acceleration), V (velocity), D (displacement) and $m = a, v, d$. Finally, a straight line is fitted between log10(PGM) and log10(Pm3) with standard error

installed in the seismically active region of Kachchh, Gujarat.

Encouraged by the performance and working of EEW in the Himalayas, ISR as a pilot project has begun building the EEW system for urban areas like Ahmedabad from earthquakes originating in Kachchh region. ISR is planning to install a network of EEW instruments in eastern Kachchh region of Gujarat, India. A lot of work has been done to see the applicability of the EEW system for this region. Peak ground acceleration (PGA), peak ground velocity (PGV), and peak ground displacement (PGD) are routinely used parameters to define the strength of shaking. In the present work, several relationships between various parameters like PGA, PGV, PGD, P_a, P_v, and P_d have been estimated using GSNet data. The main focus is kept on estimating P_d and τ_c values, which are crucial in deciding the magnitude of an earthquake and ultimately the severity of an earthquake. These parameters play a key role in issuing the EEW warning.

Seismotectonics of Kachchh region

Broadly, Gujarat is divided into three divisions, namely Saurashtra, Kachchh, and Mainland Gujarat. Gujarat geology is the outcome of various climatic and igneous activities. Gujarat structure is divided into two parts, namely Precambrian structural trends and Mesozoic structural trends. Precambrian basement is overlain by younger rocks of Jurassic, Cretaceous, Tertiary, and Quaternary

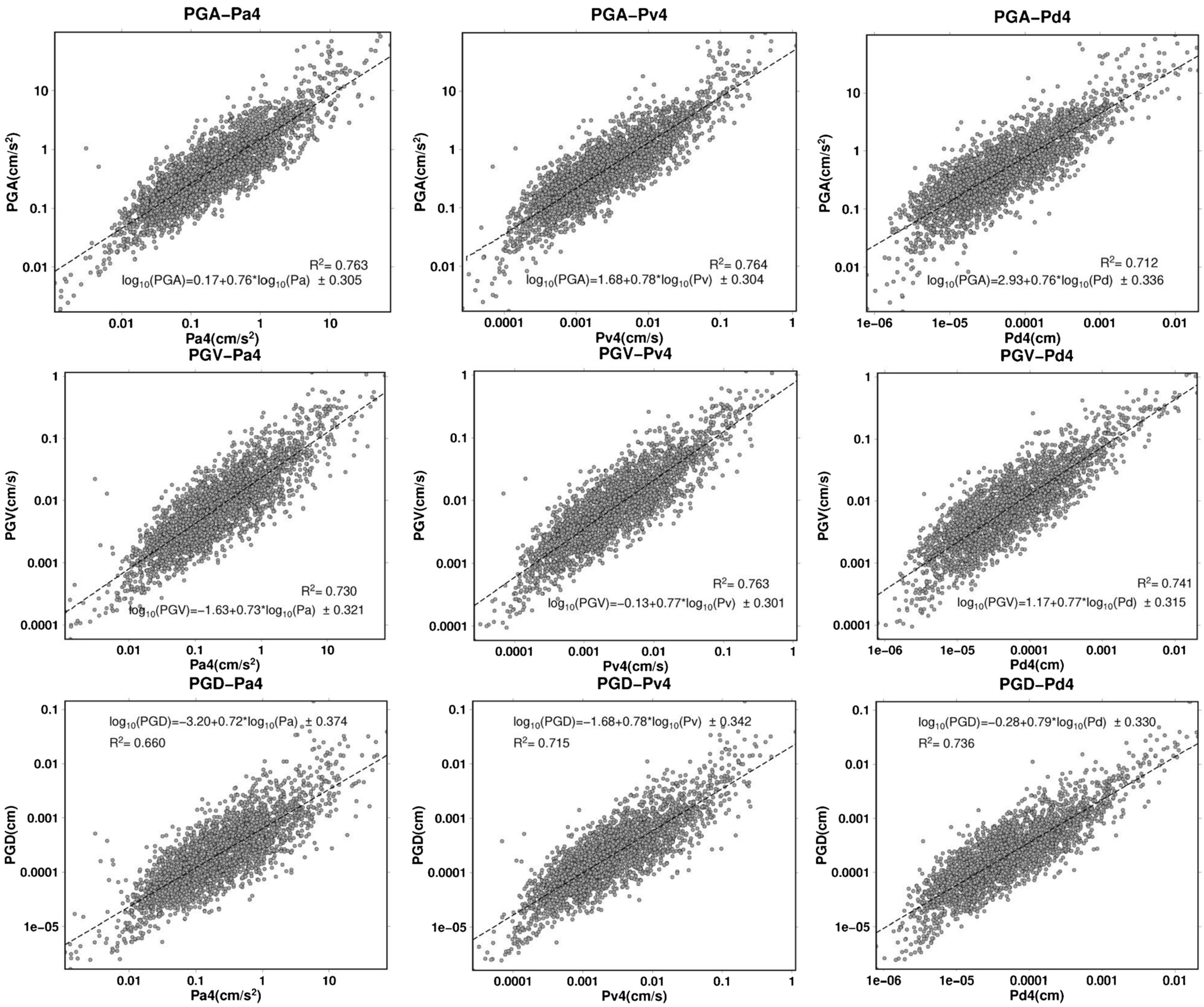

Fig. 4 Empirical relationships between ground motion parameters (PGA, PGV, PGD, P_a, P_v, P_d) for 4-s window after P-wave arrival

periods (Biswas 1987, 2005; Merh 1995). Deccan basalt covers the major parts of Saurashtra, South Gujarat, and some portions of Kachchh with intervening Cretaceous and Tertiary rocks at many places.

Narmada, Kachchh, and Cambay are the three marginal rifts which form an integral part of Gujarat with the presence of many active faults (Biswas 1987, 2005; Talwani and Gangopadhyay 2001). The faults in these rifts follow important tectonic trends, viz. Kachchh basin in Delhi trend, the Narmada in Satpura trend, and Cambay basin in Dharwar trend. The Kachchh region is occupied with pre-Quaternary rocks (Gupta et al. 2001) and is characterized by uplifted highlands and islands surrounded by plains of the Great Rann, Banni, and Little Rann. The mainland Kachchh is a rocky terrain with northern hill range and Katrol hill range bounded in their north by a fault. The tilted block uplifts in the region are caused by sub-parallel faults. From north to south, uplifts are bounded by different faults, namely Nagar Parkar Fault (NPF), Allah Bund Fault (ABF), Island Belt Fault (IBF), Kutch Mainland Fault (KMF), and South Wagad Fault (SWF). The northern hill range is bounded by major faults, namely the Kachchh Mainland Fault (KMF) and Katrol Hill Fault (KHF). The most strained region is where KMF overhangs the South Wagad Fault (SWF) (Biswas 2005). The Bhuj earthquake in 2001 of M_w 7.7 that claimed around 14,000 lives was located in this Kachchh region close to KMF (Fig. 1).

Data and methodology

A total of 310 earthquakes originating from Kachchh area during 2010 to 2015 having M 3.0–5.2 have been utilized in the present analysis. These earthquakes were recorded by 27 broadband seismograph stations of GSNet (Fig. 2).

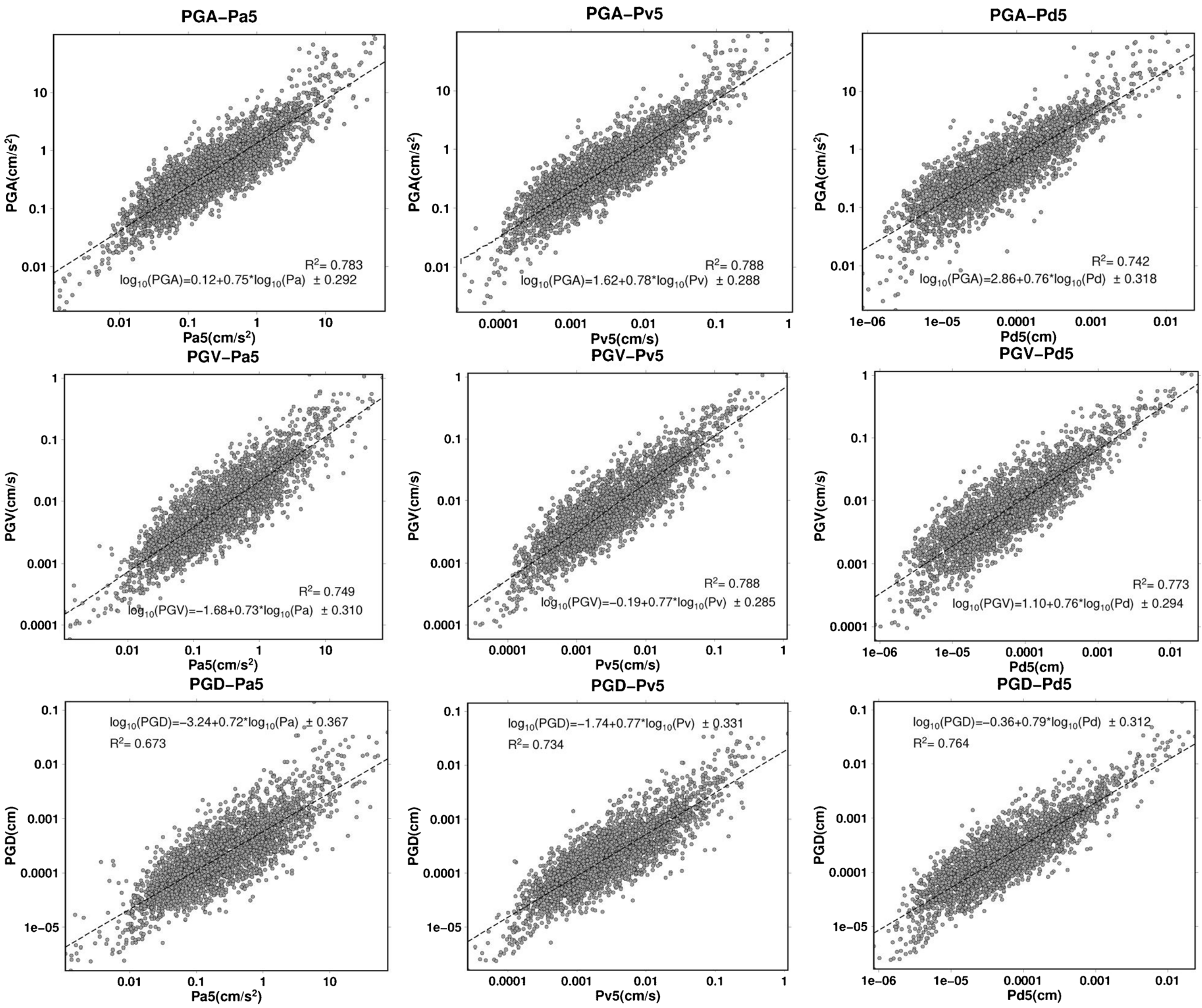

Fig. 5 Empirical relationships between ground motion parameters (PGA, PGV, PGD, P_a, P_v, P_d) for 5-s window after P-wave arrival

All the seismographs are equipped with 120-s CMG-3T broadband sensor with 24-bit recorder. The stations record ground motion velocity continuously at 100 samples per second. A total of 2986 records with an epicentral distance less than 100 km have been used in this study. Each seismogram is first corrected for instrument response and then differentiated to get acceleration and integrated for displacement. A 0.075 Hz high-pass recursive Butterworth filter is applied to remove low frequency drift caused by the integration process. Since we are dealing with the initial portion of the waveform, using high-pass filter will not cause any effect on estimating parameters. From the first 3 s, 4 s, and 5 s of the P-phase of vertical acceleration, velocity, and displacement time series, we estimated the maximum acceleration (P_a), velocity (P_v), and displacement (P_d) respectively. Peak ground acceleration (PGA), velocity (PGV), and displacement (PGD) are picked from the larger ground motion of the two horizontal components. We used the P-wave to estimate the overall size of an earthquake. Both P- and S-waves are generated due to the seismic fault motion, but the amplitude of P-wave is, on average, much smaller than the amplitude of S-wave. For a point double-couple source, the ratio of the maximum P-wave amplitude to that of the S-wave is approximately 0.2. Thus, the S-wave is primarily responsible for damage owing to the earthquake. However, the waveform of the P-wave reflects how the slip on the fault plane is occurring. As P-wave carries information and S-wave carries energy, so by observing the P-wave over some time, we can have source information during this time. It is obvious that a longer average time period (τ_0) would provide more accurate information of the source. However, if τ_0 is too long, the early warning merit of the method is compromised. The following method is used to

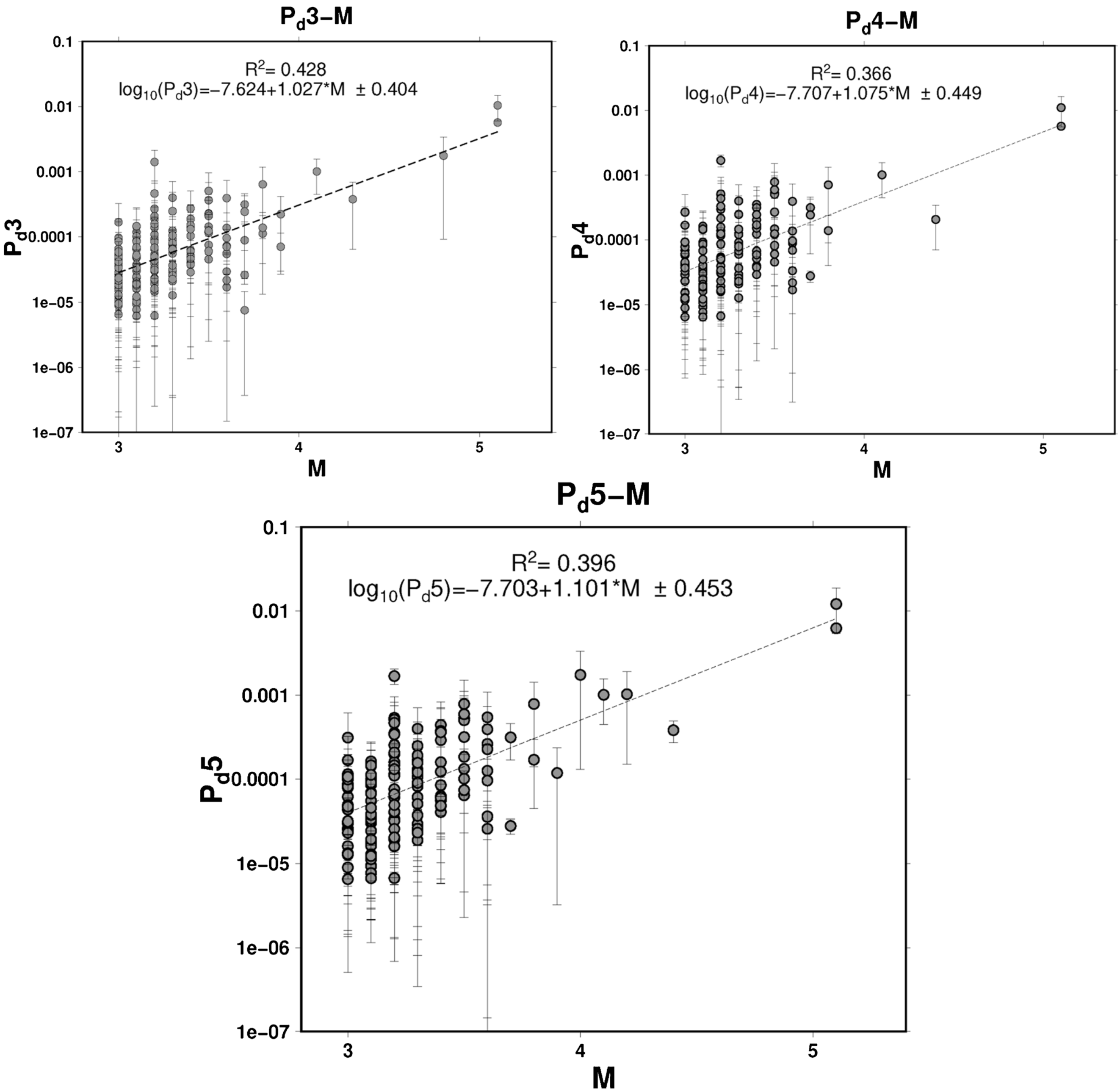

Fig. 6 Empirical relationships between P_d and M for different time windows (3–5 s) after P-wave arrival. Following Kanamori (2005) and Wu and Kanamori 2005a, 2005b), average P_d and its standard deviation are calculated for each event. Then, Pearson correlation coefficient (regression coefficient) is calculated between log10(P_d) and magnitude (M). Finally, a straight line is fitted between log10(P_d) and M with standard error

estimate various parameters modified after Nakamura (1988) and proposed by Wu and Kanamori (2005a).

$$r = \frac{\int_0^{\tau_0} u^2(t)dt}{\int_0^{\tau_0} u^2(t)dt} \tag{1}$$

where $u(t)$ is displacement and is obtained by integrating over some time, typically 3 s after P-wave arrival. Using Parseval's theorem,

$$r = \frac{4\pi^2 \int_0^{\infty} f^2 \left|\hat{u}(f)\right|^2 df}{\int_0^{\infty} \left|\hat{u}(f)\right|^2 df} = 4\pi^2 \langle f^2 \rangle \tag{2}$$

where f is the frequency, $\hat{u}(f)$ is the frequency spectrum of $u(t)$ and $\langle f^2 \rangle$ is the average of f^2 weighted by $|\hat{u}(f)|^2$. Then, τ_c is given as below:

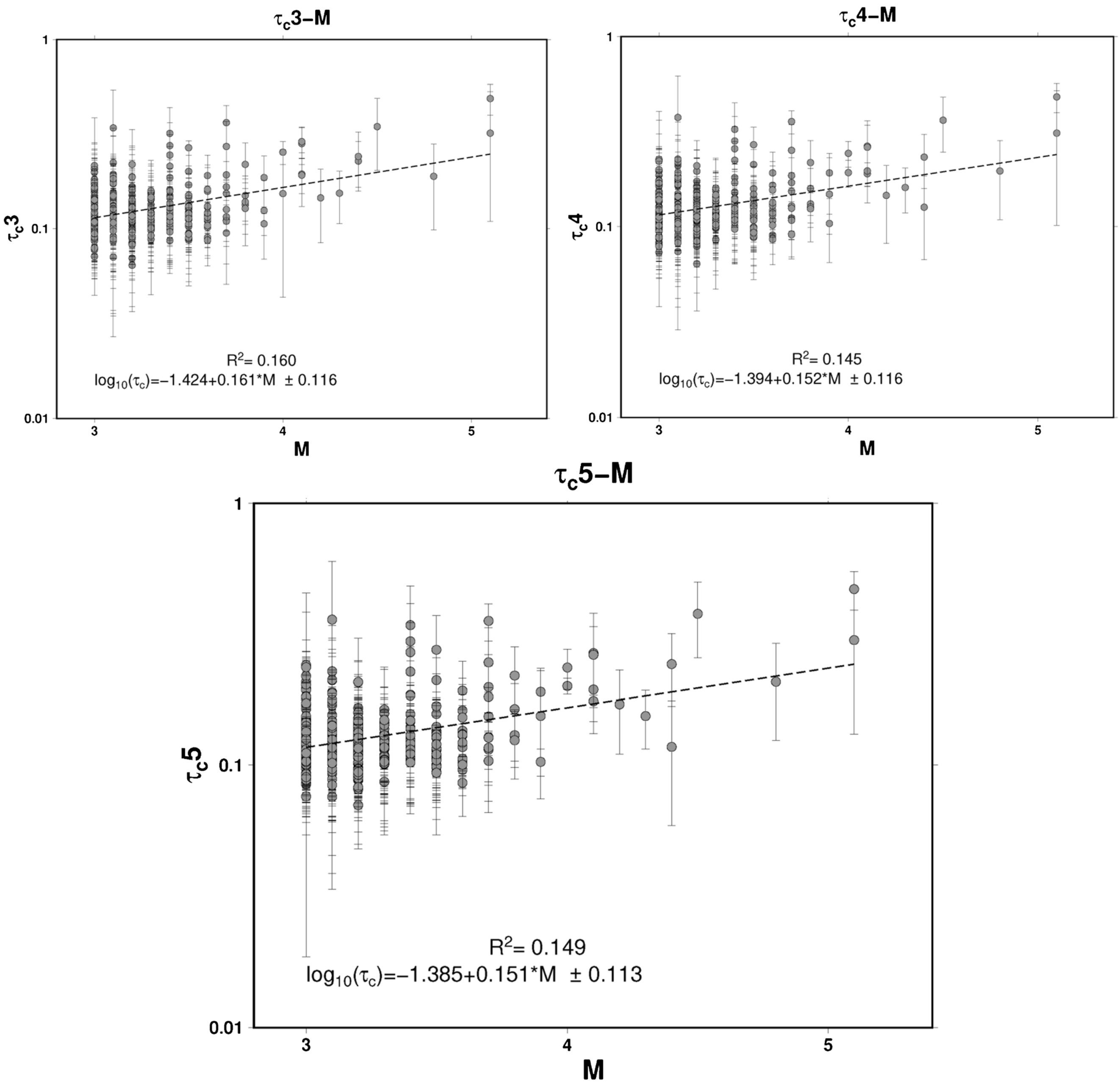

Fig. 7 Empirical relationships between τ_c and M for different time windows (3–5 s) after P-wave arrival. Following Kanamori (2005) and Wu and Kanamori (2005a, 2005b)), average τ_c and its standard deviation are calculated for each event. Then, Pearson correlation coefficient (regression coefficient) is calculated between log10(τ_c) and magnitude (M). Finally, a straight line is fitted between log10(τ_c) and M with standard error

$$\tau_c = \frac{1}{\sqrt{\langle f^2 \rangle}} = \frac{2\pi}{\sqrt{r}} \tag{3}$$

This parameter is used to represent the period of the waveform. τ_c estimated from initial few seconds typically 3 s is used to estimate magnitude for events ≤ 6. However, for the events ≥ 6.5, the magnitude can be estimated using τ_c from greater time windows. This procedure takes longer time and may not be practical for nearby cities (Wu and Kanamori 2005b). τ_c estimation uses the frequency content of P-wave while another parameter P_d adopts the amplitude content of the initial part of waveforms. Displacement is estimated from velocity using the integration process with a cutoff frequency of 0.075 Hz. In the same way, acceleration is estimated from velocity using differentiation. Finally, P_d, P_v, and P_a are estimated from initial 3 s, 4 s, and 5 s after the P-wave arrival.

Table 2 Comparison of regression relations obtained in the present study with regression relations established by other researchers using different datasets

Place	EEW parameters		Regression equations	References
Southern California	τ_p^{max}-M		$M_w = 7\,log\left(\tau_p^{max}\right) + 5.9$	Allen and Kanamori (2003)
Taiwan	τ_c-M		$M_w = 4.525 \quad log\ (\tau_c) + 5.036$	Wu and Kanamori (2005a)
Taiwan	τ_c-M; P_d-M		$M_w = 3.088 \quad log\ (\tau_c) + 5.30$ $log\ (p_d) = -3.80 + 0.72\,M - 1.44\,logR \pm 0.29$	Wu et al. (2006)
Southern California	P_d-M		$log(p_d) = -3.46 + 0.72M - 1.37\ log\ (R) \pm 0.305$	Wu and Zhao (2006)
Northern California	τ_p^{max}-M; P_d-M		$M_w = 5.22log\left(\tau_p^{max}\right) + 6.66; log(p_d) = 0.73\ M_w - 3.77$	Wurman et al. (2007)
Taiwan, Southern California, and Japan	τ_c-M		$M_w = 3.37 \quad log\ (\tau_c) + 5.78$	Wu and Kanamori (2008a)
Japan	τ_p^{max}-M;P_d-M		$log\left(\tau_p^{max}\right) = 0.21M_L - 1.22; log(p_d) = 0.66M_L - 4.02$	Brown et al. (2009)
Japan, Taiwan and, Central Italy	τ_c-M		$log(\tau_c) = 0.21(\pm 0.01)M_w - 1.2$	Zollo et al. (2010)
Istanbul	τ_c-M		$log(\tau_c) = 0.142M_w - 0.475 \pm 0.1433$	Alcik et al. (2011)
Taiwan	P_d-M	10 s	$log_{10}(P_d\ ) = -1.741 + 0.55 * M - 1.285\ log\ (R) \pm 0.252$	Chen et al. (2017)
Gujarat, India	P_d-M τ_c-M	3 s	$log_{10}(P_d\ ) = -7.624 + 1.027 * (M) \pm 0.404$ $log_{10}(\tau_c\ ) = -1.424 + 0.161 * (M) \pm 0.116$	Present work
Gujarat, India	P_d-M τ_c-M	4 s	$log_{10}(P_d\ ) = -7.707 + 1.075 * (M) \pm 0.449$ $log_{10}(\tau_c\ ) = -1.394 + 0.152 * (M) \pm 0.155$	Present work
Gujarat, India	P_d-M τ_c-M	5 s	$log_{10}(P_d\ ) = -7.703 + 1.101 * (M) \pm 0.453$ $log_{10}(\tau_c\ ) = -1.385 + 0.151 * (M) \pm 0.113$	Present work

Results and discussion

Following the data analysis by Wu and Kanamori (2005a), the vertical velocity time history is integrated to obtain displacement and a high-pass 0.075 Hz Butterworth filter is applied to avoid noise. In a similar way, velocity time history is differentiated to obtain acceleration time history. Instead of fixing a single time window, we choose to work for three-time windows, i.e., 3 s, 4 s, and 5 s. τ_c and P_d are estimated from the earthquakes recorded in Kachchh region having magnitude range 3–5.2. Linear regression analysis is performed at various time steps (3- to 5-s time interval) to find the various empirical relationships.

The various ground motion parameters (PGA, PGV, and PGD) are plotted against estimated parameters (P_a, P_v, *and* P_d) for three different time windows (3–5 s). The results show 1:1 correlation between PGA: P_a, PGV:P_v, and PGD:P_d. PGA and estimated P_v values are found in a proportion of 1:100, while PGA and $P_d$values show 1:1000 proportion. Similarly, PGV and $P_d$show 1:100 proportion. We observe that P_a, P_v, and P_d correlate well with peak amplitude parameters, and the highest correlation is observed for 5-s time window. Particularly, P_v and P_d are more correlated with PGA than P_a. Also, P_v and P_d have more long-period energy than P_a and correlate better with PGV. For 3- and 4-s window, some difference in values is observed. From here, it can be concluded that 5 s after the occurrence of earthquake, maximum peak values (P_a, P_v, *and* P_d) have been observed. Having 1:1 correlation between P_a and PGV, P_v and PGV, and P_d and PGD strengthens our viewpoint to use initial few seconds of waveform for magnitude estimation.

The proposed linear relationship between various parameters is of the following type:

$$log_{10}(PGA/PGV/PGD\ ) = A + B{*}log_{10}(P_a/P_v/P_d) \pm C$$

where A and B are constants to be determined through regression analysis and C is a standard error in the estimate.

Using the above guidelines, the various estimated relationships for different time windows (3–5 s) between different parameters are given in Table 1. Also, the relations plotted for 3-s, 4-s, and 5-s window are given in Figs. 3, 4, and 5 respectively.

The values of τ_c and P_d shift contrastingly for different time windows (3–5 s). In general, the value of P_d varies between 8e−07 to 0.04 cm. The values estimated from the present dataset are lower compared with the expected one. The value of P_d shows more scatter for 3-s window compared with 4- and 5-s window. Secondly, P_d values estimated from 3-s window are less in comparison with other higher time windows. For events with magnitude ≥ 6, the value of P_d using Taiwan and global data is 0.35 cm (Wu and Kanamori 2005a). P_d of vertical displacement in the first several seconds after the arrival of the P-wave have been studied in different parts of the world (Wu et al. 2007; Wu and Kanamori 2008a, 2008b, 2005b; Zollo et al. 2006; Chen et al. 2017; Mittal et al. 2019b) and reflects the attenuation relationship with distance as a function of magnitude and is also well correlated with the peak ground velocity (PGV).

The proposed regression analysis between magnitude (M) and P_d is:

$$\log_{10}(P_d) = A + B * (M) \pm C$$

The plot between M and P_d for 3–5 s is given in Fig. 6.

The values of τ_c for different time windows vary from .04 to 0.6. In the same way as P_d, the values of τ_c for 3-s window are more scattered compared with higher time windows. For most events with $M > 5$ in Taiwan, τc is ≥ 1 s, while the same value of τ_c is obtained for the events with $M > 6$ in Southern California. In our case, even some of the earthquakes have magnitude ≥ 5, but the values of τ_c are not even close to 1. This may be due to the difference in signal to noise (S/N) ratio, especially for smaller earthquakes. This difference in τ_c values is expected to decrease as the event size increases (Wu et al. 2007). But in most of the cases, it may not be a reliable EEW parameter owing to S/N sensitivity.

In a similar way, the proposed regression analysis between magnitude (M) and τ_c is:

$$\log_{10}(\tau_c) = A + B * (M) \pm C$$

Using above guidelines, the estimated relationships for different time windows (3–5 s) between τ_c and M are plotted in Fig. 7 and summarized in Table 1.

A better correlation is observed between P_d and M in comparison with τ_c and M. The correlation is better if a 5-s time window is considered. So in our viewpoint, the τ_c cannot be considered as one of the reliable EEW parameter for Kachchh region using data from GSNet. For practical early warning purposes, we are concerned with the events with $M > 6$. For estimating the magnitude of bigger earthquakes in a reliable way, different time windows need to be used after P-wave arrival. In recent time, Chen et al. (2017) used 10 different time windows (1–10 s) to estimate the magnitude of bigger earthquakes. They concluded that larger time windows are needed for estimating the magnitude efficiently using P_d methodology, but at the cost of reducing EEW warning time. Mittal et al. (2019b) used P_d methodology in India to find the magnitude of earthquakes. They used recorded earthquakes from Taiwan having magnitude close to 6. In addition, they used synthesized data for two historical earthquakes. Their estimated P_d values are in agreement with others (e.g., Chen et al. 2017; Wu et al. 2016), which confirms the applicability of P_d methodology in India. A comparison of present findings with others in the world is shown in Table 2. However, using data in the present work, this comparison may not be valid due to non-availability of higher magnitude earthquakes. ISR will be using the global data of $M > 6.0$ for fine tuning the estimated relationships and comparison in future.

Conclusion

We investigated correlations between various ground motion parameters like PGA, PGV, PGD, P_a, P_v, P_d, and τ_c using broadband data of GSNet having a magnitude range 3–5.2, operated by the Institute of Seismological Research (ISR), and showed 1:1 correlation. This correlation strengthens the basis that the initial few seconds of the waveform can be used to infer the important information about earthquakes. Three- to 5-s time windows are considered to measure P_a, P_v, P_d, and τ_c from the vertical component of the waveforms. In Gujarat, the stations of Gujarat State Seismic Network are not densely distributed all over the Kachchh region. Earthquake early warning system for far away cities of Gujarat is possible with earthquake occurring in the eastern part of Gujarat with the dense network. ISR is going to install about 50 SMA in Kachchh region of Gujarat to have a denser network. So if detection of the P arrival and τ_c and P_d estimations are done within 15 s, then early warning may be provided to the cities around 70 km or more from epicenter. Also by that time, S-waves carrying destructive waves have travelled 60 km from the epicenter, so warning is possible for regions beyond 60 km. A better correlation is observed between P_d and M in comparison with τ_c and M. The correlation is better if a 5-s time window is considered. So in our viewpoint, the τ_c cannot be considered as one of the reliable EEW parameters for Kachchh region using data from GSNet owing sensitivity of τ_c to signal to noise ratio. Due to earthquakes of $M > 6.0$, VSAT systems may be disturbed, so use of fiber cable for transmitting the data is preferable. However, τ_c and P_d methods may overcome this difficulty because τ_c and P_d are measured from the beginning of P arrival, before telemetry interruption occurs.

Acknowledgments This manuscript is prepared under collaborative project by India and Taiwan. The authors are thankful to the Director General (DG) and Director, Institute of Seismological Research (ISR), for giving necessary permission to use the ISR data. The authors thankfully acknowledge the three reviewers and associate editor for their constructive comments, which helped in improving the manuscript.

Funding information During this collaborative work, all the financial support was from the Department of Science and Technology, New Delhi, India, the National Taiwan University (NTU), and the Ministry of Science and Technology (MOST), Taiwan.

References

Alcik H, Ozel O, Wu YM, Ozel NM, Erdik M (2011) An alternative approach for the Istanbul earthquake early warning system. Soil Dyn Earthq Eng 31(2):181–187

Allen RM, Kanamori H (2003) The potential for earthquake early warning in Southern California. Science 300:685–848

Allen RM, Gasparini P, Kamigaichi O, Böse M (2009) The status of earthquake early warning around the world: an introductory

overview. Seismol Res Lett 80(5):682–693. https://doi.org/10.1785/gssrl.80.5.682
Anderson J, Quaas R, Singh SK, Manuel Espinosa J, Jiminez A, Lermo J, Cuenca J, Sanchez-Sesma F, Meli R, Ordaz M, Alcocer S, Lopez B, Alcantara L, Mena E, Javier C (1995) The Copala, Guerrero, Mexico earthquake of September 14, 1995 (Mw 7.4): a preliminary report. Seismol Res Lett 66:11–39
Biswas SK (1987) Regional tectonic framework, structure and evolution of western marginal basins of India. Tectonophysics 135:307–327
Biswas SK (2005) A review of structure and tectonics of Kutch basin, western India with special reference to earthquakes. Curr Sci 88: 1592–1600
Brown HM, Allen RM, Grasso VF (2009) Testing alarms in Japan. Seismol Res Lett 80(5):727–739
Chen DY, Wu YM, Chin TL (2015) Incorporating low-cost seismometers into the Central Weather Bureau seismic network for earthquake early warning in Taiwan. Terr Atmos Ocean Sci 26:503–513. https://doi.org/10.3319/TAO.2015.04.17.01(T)
Chen DY, Wu YM, Chin TL (2017) An empirical evolutionary magnitude estimation for early warning of earthquakes. J Asian Earth Sci 135:190–197
Chopra S, Yadav RBS, Patel H, Kumar S, Rao KM, Rastogi BK, Hameed A, Srivastava S (2008) The Gujarat (India) Seismic Network. Seisml Res Lett 79(6):806–815
Espinosa-Aranda JA, Jimenez A, Ibarrola G, Alcantar F, Aguilar A, Inostroza M, Maldonado S (1995) Mexico City seismic alert system. Seismol Res Lett 66:42–53
Gupta HK, Rao NP, Rastogi BK, Sarkar D (2001) The deadliest intraplate earthquake. Science 291:2101–2102
Hoshiba M, Kamigaichi O, Saito M, Tsukada SY, Hamada N (2008) Earthquake early warning starts nationwide in Japan. EOS Trans Am Geophys Union 89(8):73–74
Johnston AC, Kanter LR (1990) Earthquakes in stable continental crust. Sci Am 262:68–75
Kamigaichi O, Saito M, Doi K, Matsumori T, Tsukada SY, Takeda K, Shimoyama T, Nakamura K, Kiyomoto M, Watanabe Y (2009) Earthquake early warning in Japan: warning the general public and future prospects. Seismol Res Lett 80(5):717–726
Kanamori H (2005) Real-time seismology and earthquake damage mitigation. Annu Rev Earth Planet Sci 33:195–214
Kumar A, Mittal H, Sachdeva R, Kumar A (2012) Indian strong motion instrumentation network. Seismol Res Lett 83(1):59–66
Kumar A, Mittal H, Chamoli BP, Gairola A, Jakka RS, Srivastava A (2014). Earthquake early warning system for Northern India. 15th Symposium on Earthquake Engineering, Indian Institute of Technology, Roorkee, Dec 11–13, 2014: 231–238, New Delhi: Elite Publishing.
Lockman A, Allen RM (2005) Single station earthquake characterization for early warning. Bull Seismol Soc Am 85:2029–2039
Merh SS (1995). Geology of Gujarat. Geol. Soc. Bangalore, 224p.
Mittal H, Gupta S, Srivastava A, Dubey RN, Kumar A (2006) National strong motion instrumentation project: an overview. In: In 13th Symposium on Earthquake Engineering, Indian Institute of Technology, Roorkee. Elite Publishing, New Delhi, pp 107–115
Mittal H, Kumar A, Wu YM, Kumar A (2016a) Source study of M w 5.4 April 4, 2011 India–Nepal border earthquake and scenario events in the Kumaon–Garhwal Region. Arab J Geosci 9(5):348
Mittal H, Wu YM, Chen DY, Chao WA (2016b) Stochastic finite modeling of ground motion for March 5, 2012, Mw 4.6 earthquake and scenario greater magnitude earthquake in the proximity of Delhi, Nat. Hazards 82(2):1123–1146. https://doi.org/10.1007/s11069-016-2236-x
Mittal H, Wu YM, Lin TL, Legendre CP, Gupta S, Yang BM (2019a) Time-dependent shake map for Uttarakhand Himalayas, India, using recorded earthquakes. Acta Geophysica 67(3):753–763
Mittal H, Wu YM, Sharma ML, Yang BM, Gupta S (2019b) Testing the performance of earthquake early warning system in northern India. Acta Geophysica 67(1):59–75
Nakamura Y (1988). On the urgent earthquake detection and alarm system (UrEDAS), Proceeding of 9th World Conference on Earthquake Engineering, Tokyo-Kyoto, Japan.
Olson EL, Allen RM (2005) The deterministic nature of earthquake rupture. Nature 438:212–215
Quittmeyer RC, Jacob KH (1979) Historical and modern seismicity of Pakistan, Afghanistan, northwestern India, and southeastern Iraq. Bull Seismol Soc Am 69(3):773–823
Rastogi BK (2001) Ground deformation study of Mw 7.7 Bhuj earthquake of 2001. Episode 24(3):160–165
Rastogi BK (2004) Damage due to the Mw7.7 Kutch, India earthquake of 2001. Tectonophysics 390:85–103
Talwani P, Gangopadhyay A (2001) Tectonic framework of the Kachchh earthquake of January 26, 2001. Seismol Res Lett 72:336–345
Wu YM, Kanamori H (2005a) Experiment on an onsite early warning method for the Taiwan early warning system. Bull Seismol Soc Am 95(1):347–353
Wu YM, Kanamori H (2005b) Rapid assessment of damaging potential of earthquakes in Taiwan from the beginning of P waves. Bull Seismol Soc Am 95:1181–1185
Wu YM, Kanamori H (2008a) Exploring the feasibility of on-site earthquake early warning using close-in records of the 2007 Noto Hanto earthquake. Earth Planets Space 60:155–160
Wu YM, Kanamori H (2008b) Development of an earthquake early warning system using real-time strong motion signals. Sensors 8:1–9
Wu YM, Zhao L (2006) Magnitude estimation using the first three seconds P-wave amplitude in earthquake early warning. Geophys Res Lett 33:L16312
Wu YM, Shin TC, Tsai YB (1998) Quick and reliable determination of magnitude for seismic early warning. Bull Seismol Soc Am 88: 1254–1259
Wu YM, Yen HY, Zhao L, Huang BS, Liang WT (2006) Magnitude determination using initial P waves: a single-station approach. Geophys Res Lett 33(5):L05306. https://doi.org/10.1029/2005GL025395
Wu YM, Kanamori H, Richard MA, Hauksson E (2007) Determination of earthquake early warning parameters, τc and P_d, for southern California. Geophys J Int 170:711–717. https://doi.org/10.1111/j.1365-246X.2007.03430.x
Wu YM, Chen DY, Lin TL, Hsieh CY, Chin TL, Chang WY, Li WS, Ker SH (2013) A high density seismic network for earthquake early warning in Taiwan based on low cost sensors. Seismol Res Lett 84:1048–1054. https://doi.org/10.1785/0220130085
Wu YM, Liang WT, Mittal H, Chao WA, Lin CH, Huang BS, Lin CM (2016) Performance of a low-cost earthquake early warning system (P-alert) during the 2016 ML 6.4 Meinong (Taiwan) earthquake. Seismo Res Let 87(5):1050–1059. https://doi.org/10.1785/0220160058
Wu YM, Mittal H, Huang TC, Yang BM, Jan JC, Chen SK (2019) Performance of a Low-Cost Earthquake Early Warning System (P-Alert) and shake map production during the 2018 Mw 6.4 Hualien (Taiwan) Earthquake. Seismo Res Lett 90(1):19–29. https://doi.org/10.1785/0220180170
Wurman G, Allen RM, Lombard P (2007) Toward earthquake early warning in northern California. J Geophys Res Solid Earth 112(B8)
Zollo A, Lancieri M, Nielsen S (2006) Earthquake magnitude estimation from peak amplitudes of very early seismic signals on strong motion records. Geophys Res Lett 33:L23312. https://doi.org/10.1029/2006GL027795
Zollo A, Amoroso O, Lancieri M, Wu YM, Kanamori H (2010) A threshold-based earthquake early warning using dense accelerometer networks. Geophys J Int 183(2):963–974